RANKL and OPG activity is regulated by injury size in networks of osteocyte-like cells

Lauren E. Mulcahy, David Taylor, T. Clive Lee, Garry P. Duffy

PII: S8756-3282(10)01459-6
DOI: doi: 10.1016/j.bone.2010.09.014
Reference: BON 8998

To appear in: *Bone*

Received date: 10 May 2010
Revised date: 8 September 2010
Accepted date: 8 September 2010

Please cite this article as: Mulcahy Lauren E., Taylor David, Lee T. Clive, Duffy Garry P., RANKL and OPG activity is regulated by injury size in networks of osteocyte-like cells, *Bone* (2010), doi: 10.1016/j.bone.2010.09.014

RANKL and OPG activity is regulated by injury size in networks of osteocyte-like cells

Lauren E. Mulcahy [1,2 *]
David Taylor[1]
T. Clive Lee [1,2]
Garry P. Duffy [1,2]

[1]*Trinity Centre for Bioengineering, Department of Mechanical Engineering, Dublin 2, Ireland*
[2]*Department of Anatomy, Royal College of Surgeons in Ireland, St. Stephen's Green, Dublin 2, Ireland*

Word Count: 4305

Key Words: Bone Homeostasis, RANKL, OPG, Bone remodelling, Microcracks

Lauren Mulcahy, BSc, MSc
Trinity Centre for Bioengineering,
Department of Mechanical Engineering,
Dublin 2,
Ireland.
+353 1 8961703.
mulcahle@tcd.ie
*corresponding author

Department of Anatomy,
Royal College of Surgeons in Ireland,
123 St. Stephens Green,
Dublin 2.
+353 1 4022147
laurenmulcahy@rcsi.ie

David Taylor, MA, PhD, ScD, FTCD, FIEI, CEng
Trinity Centre for Bioengineering,
Department of Mechanical Engineering,
Dublin 2,
Ireland
+353 1 8961703
dtaylor@tcd.ie

T. Clive Lee, MD, PhD (Dubl), FRCSI, FRCSEd, CEng, FIEI
Department of Anatomy,
Royal College of Surgeons in Ireland,
123 St. Stephens Green.
Dublin 2.
+353 1 4022264
tclee@rcsi.ie

Garry Duffy, PhD
Department of Anatomy,
Royal College of Surgeons in Ireland,
123 St. Stephens Green,
Dublin 2.
+353 1 4022105
garryduffy@rcsi.ie

Abstract

Bone remodelling is an intricate process encompassing numerous paracrine and autocrine biochemical pathways and mechanical mechanisms. It is responsible for maintaining bone homeostasis, structural integrity and function. The RANKL-RANK-OPG cytokine system is one of the principal mediators in the maintenance of bone cell function and activation of bone remodelling by the Basic Multicellular Unit (BMU) which carries out remodelling. Theories surrounding the initiation of bone remodelling include mechanical loading, fluid flow and microdamage as potential stimuli. This study focused on microdamage. In an *in vitro* simulated bone environment, gel embedded MLO-Y4 cell networks were subjected to damage in the form of planar, crack-like defects of constant area and varying thickness. The biochemical response was determined by ELISA and luciferase assay. The results showed that RANKL release increased and OPG decreased in a manner which depended on injury size (i.e. thickness) and time following application of injury. The effect of microdamage on cell viability and apoptosis was also evaluated. This work demonstrates that injury alone, in the absence of imposed strain or fluid flow, is sufficient to initiate changes in cytokine concentrations of the type which are known to stimulate bone remodeling.

Introduction.

Bone is a dynamic material which is continuously being remodelled in order to maintain calcium homeostasis and to preserve volume. Bone remodelling is controlled by the Basic Multicellular Unit (BMU), which requires a tightly coordinated grouping of osteocytes, osteoblasts and osteoclasts. The contributing elements in the functioning of bone homeostasis are regulated hierarchically through a series of cell signals, cross talk and cascades, essentially focused on members of the tumour necrosis factor superfamily- Receptor Activator of NFκ B Ligand (RANKL) and its receptors, Receptor Activator of NFκ B (RANK) and Osteoprotegrin (OPG) [1, 2] These, along with other factors, such as ephrins and interleukins, are central mediators of differentiation, proliferation and inhibition of osteoclasts, and are pivotal in the bone remodelling process [3, 4].

Osteocytes, which constitute 90-95% of all bone cells, being present in quantities of 12,000-25,000 cells per mm^3, form intricate cell process networks *via* cellular processes (typically 50-100 processes per cell) which penetrate canaliculi in the bone matrix [5-7]. Osteocytes are believed to be capable of mechanotransduction, allowing them to detect alterations in matrix strain and canalicular fluid flow [8].

Microdamage in bone is a naturally occurring phenomenon resulting from daily cyclic loading, which can manifest itself as ellipsoidal cracks, normally ranging from 50-400μm in width, measured transverse to the bone's axis. A build up of microcracks in bone is a factor in reduced strength [9]. Force and loading on a bone has been found to elicit DNA damage in osteocytes proportional to the force applied [10]. It has long been thought that microdamage in bone is one of the principal mediators of bone remodelling and in the initiation of the BMU, which then functions in removing damaged or compromised bone surrounding [11-13]. It has been found that the birth rate and longevity of the BMU is directly proportional to the frequency and intensity of microcracks and that mechanical stimulus is a major contributing factor to the dedifferentiation process of osteocytes into osteoblasts [14].

It has been established that the RANKL-RANK-OPG signaling pathway is greatly involved in the activation of bone remodelling by the BMU. RANKL is a primary mediator in the activation and differentiation of preosteoclasts into osteoclasts, and so

functions in stimulating and sustaining bone remodelling [15, 16]. RANKL has been shown to be induced by numerous factors, including parathyroid hormone tumour necrosis factor alpha (TNF), TGF α, 1, 25 dihydroxyvitamin D3, prostaglandin E_2 (PGE_2), interleukin 1 (IL-1), interleukin 6 (IL-6) and interleukin 11 (IL-11)[17-19]. Osteoclast activation occurs as a result of RANKL binding to the RANK receptor on the cell surface of preosteoclasts and mature osteoclasts [1, 20-22].

RANKL is antagonised by OPG, a member of the TNF superfamily, which functions by binding to and sequestering RANKL, impeding the resorption of bone [1, 23, 24] .OPG is released from the osteoblast lineage of cells on receipt of signals such as oestrogen, BMPs and TGF-β [21]. OPG blocks receptor function of RANKL through alteration of orientation and by blocking cytoplasmic interactions and NFκ B activation [25].

There is strong evidence to suggest that remodeling is targeted to regions containing microcracks [11] implying that the osteocyte network is capable of detecting them. As yet, the mechanism of detection is unclear, though some workers have suggested that this could be done via the cells' mechanotransduction capabilities [26]. We have proposed an alternative mechanism, by which cellular processes spanning the crack could be ruptured by a shearing mechanism similar to the action of a pair of scissors [27-29].

To understand the bone remodelling response to microdamage, a microenvironment using an osteocyte cell line (MLO-Y4) seeded in collagen-matrigel constructs was developed. MLO-Y4 cells have been shown to have many characteristics of osteocytes, predominantly, similar phenotype in a stellate morphology, and the ability to produce large amounts of osteocalcin and type 1 collagen. MLO-Y4 cells were cultured in collagen/matrigel composite gels which facilitated the formation of cell-cell process networks similar to those seen *in vivo*. Crack-like planar defects were created in the gel embedded cells, and the biochemical response quantified by ELISA and luciferase assay. The objective of this study was to determine the effect of microdamage on RANKL and OPG release and to quantify this effect as a function of the severity of the damage applied.

Methods

Cell Culture

MLO-Y4 cells were maintained in α Modified Eagles medium (Biosera) supplemented with 5% fetal bovine serum (Biosera), 5% iron supplemented calf serum and 1% antibiotics (penicillin/ streptomycin) (Sigma Aldrich). Cells were cultured in collagen coated flasks (0.15 mg/mL rat tail collagen type 1) at 37 °C at 5% CO_2. They were passaged every 2-3 days at 80% confluency.

Three dimensional MLO-Y4 culture

In order to simulate a 3D *in vitro* bone micro-environment, MLO-Y4 cells were embedded in a 3D rat tail collagen type I /Matrigel construct (BD Biosciences). Constructs were prepared by the addition of 1 volume of Matrigel basement membrane matrix to 1 volume of a collagen solution comprised of 58% Collagen, 26% 5x DMEM (Sigma Aldrich), 2.5 % FBS, 2.5% CS, 5% Sodium Hydroxide (Sigma Aldrich) and 5% cell suspension. Such 3D culture ensures cell process formation from osteocytes. The collagen / Matrigel constructs containing 1 x 10^6 cells/mL of gel were cultured in 24 well plates and incubated for 1 hour prior to addition of normal growth medium[30]. They were cultured for 5 days prior to experimentation to facilitate cell process network formation.

Microinjury study of 3D gel embedded MLO-Y4 cells

In order to apply local damage to the gel embedded MLO-Y4 cells, gels were subjected to microdamage of a set length and width and variable thickness using acupuncture needles (Harmony Medical), of four different diameters: 160, 300, 400 and 800 µm. A single planar defect was created in each culture well by inserting a needle vertically into the centre of the hydrogel (see fig.1A) and drawing it through at a right angle, creating a defect with dimensions of 7 mm in length x 5 mm in depth. Negative controls were uninjured cells and hydrogels excluding cells. Gels were incubated using OptiMEM (Invitrogen) serum free media. Samples were taken at 24 hour intervals over a 72 hour

time period. RANKL and OPG were quantified by means of single sited specific ELISA (Mouse RANKL and OPG ELISA, R and D systems). n = 3 cultures were assayed at each injury level, in addition to non-injured controls.

Plasmids

A RANKL promoter construct developed by O Brien [31] was used, which contains a luciferase gene reporter downstream of the RANKL promoter, in addition to a neomycin resistance gene to ensure growth of a transfected cell population. Expression of luciferase downstream of the RANKL promoter is indicative of RANKL gene expression in the cells. This then allows for quantification of RANKL promoter activity which correlates to RANKL production. In addition to quantifying the production of RANKL from live cells and allowing the comparison between the release of cell bound RANKL from MLO-Y4 cells and RANKL gene expression, the use of the promoter construct may also indicate that some cells remain viable at the point of injury. The RANKL – luciferase plasmid was prepared in 50µl TRIS/EDTA. One Shot chemically competent E coli cells (Invitrogen) were transformed with 5 µl RANKL ligation reaction and grown overnight in 2mL LB Agar containing 100 mg/mL kanamycin (Sigma Aldrich). Plasmid cultures were isolated and grown overnight in LB broth preceding plasmid purification using Qiagen Miniprep. A 250mL overnight culture of transformed cells was cultured under shaking conditions (225 rpm) and the plasmid purified by means of Qiagen Maxiprep kit. Plasmid DNA was quantified by spectroscopy (Mason Nanodrop 1000).

Transfection of GFP plasmid

MLO-Y4 cells were grown at a density of 1 x 10^5 cells in a 24 well plate 24 hours prior to experimentation. Transfection was optimised by means of 1µg/µl green fluorescent protein (GFP) positive plasmid and were conducted using Lipofectamine 2000 (Invitrogen). 3 ratios of plasmid: lipofectamine were used to establish the best means of transfection efficiency; 1:1, 1:2 and 2:1. Plasmid DNA and lipofectamine was diluted accordingly with an appropriate quantity of optiMEM (50 µl: 50 µl lipofectamine

complex: plasmid complex) and applied to cells. Following 6 hours of incubation, the plasmid-lipofectamine solution was replaced with MLO-Y4 culture medium and incubated for 48 hours. Cells were analysed by means of fluorescent microscopy to establish the optimum transfection conditions and lipid/pDNA transfection ratios showing the greatest quantity of GFP positive cells (data not shown).

Transfection of MLO-Y4 Cells with RANKL promoter plasmid

MLO-Y4 cells were grown at a density of 1 x 10^5 cells in a 24 well plate 24 hours prior to experimentation, and cells were transfected with a plasmid containing the reporter gene luciferase under the control of the RANKL promoter. Transfections were conducted using a 2:1 ratio RANKL promoter + luciferase plasmid and lipofectamine at a concentration of 1µg/µl plasmid. Plasmid DNA and lipofectamine was diluted accordingly with an appropriate quantity of optiMEM (50 µl: 50 µl lipofectamine complex: plasmid complex) and applied to cells. Following 6 hour incubations, the plasmid-lipofectamine solution was replaced with MLO-Y4 culture medium and incubated for 48 hours. Luciferase activity was confirmed by means of a luciferase assay.

Determination of RANKL promoter activity: Luciferase Assay

Luciferase activities were measured using a luciferase reporter assay kit (Promega) followed by quantification using spectroscopy. Culture medium was removed and cells were rinsed with dPBS. 400 µl lysis reagent was added to cells followed by a 15 minute incubation. The lysis buffer was placed in a tube and incubated briefly. 20 µl of cell lysate was then added to 100 µl luciferase assay reagent and the luminescence measured with the Victor 3 Wallac 1420 multilabel centre.

Generation of cell line expressing RANKL promoter plasmid

To ensure that the RANKL promoter plasmid had integrated into the host cell genome, a neomycin selection of transfected cells was performed. The RANKL promoter plasmid contains a neomycin resistant gene which permits cells expressing the promoter to survive in neomycin enriched media. Transfected cells were plated at a density of 1×10^5 cells in a 6 well plate 72 hour prior to experimentation. 100 mg/mL neomycin (Sigma Aldrich) was added to cells following incubation under normal conditions. Media was changed every week until colonies of resistant cells became apparent, when they were incubated as normal in neomycin positive media. Expression of RANKL promoter was further verified using a luciferase reporter assay kit.

Microdamage to RANKL promoter positive MLO-Y4 embedded gels

Collagen-Matrigel constructs were set up and microinjury applied as previously described. Constructs contained MLO-Y4 cells transfected with the plasmid containing the reporter gene luciferase under the control of the RANKL promoter. Negative controls were uninjured cells and hydrogels excluding cells. Aliquots were removed at 24 hour time points over a 72 hour period. 20 µl of luciferase assay reagent was added to 100 µl aliquots of media and luminescence measured by spectroscopy to quantify release of RANKL. n = 3 cultures were assayed at each injury level, in addition to non-injured controls.

Effect of microdamage on entire cell population

An additional experiment was carried out in order to assess the effect of microdamage on cells not directly involved at the injury site. Collagen-Matrigel constructs were set up and microinjury applied as previously described. Constructs contained MLO-Y4 cells transfected with the plasmid containing the reporter gene luciferase under the control of the RANKL promoter. Conditioned media from previous experiments on non-transfected cells having received 400 µm injury at 48 (A) and 72 (B) hours was placed on

undamaged matrices for 72 hours and the production of RANKL quantified by means of luciferase assay. n = 3 cultures were assayed in each case.

Determination of cell viability and apoptosis following microdamage to gel embedded MLO-Y4 cells

To determine the effect of microdamage on cell viability and caspase 3 and 7 activity in our in vitro model, 100 µl of collagen/matrigel construct containing 1 x 10^6 cells/mL gels was cultured in a 96 well plate under conditions previously described. Microdamage was applied following a culture period of 72 hours, apoptosis and cell viability was determined using an ApoTox-Glo™ Triplex Assay (Promega), under manufacturers' instructions. This kit measures 2 independent biomarkers simultaneously to determine the effect of varying parameters on cell viability through measuring live/dead cell protease activity, in addition to caspase 3 and 7 activity for apoptosis. Briefly, media was removed from gels and incubated for 30 minutes in the viability/toxicity reagent at 37 ºC. Fluorescence was measured at $400_{EX}/505_{EM}$ to determine cell viability. 100 µl of Caspase-Glo Reagent was then added to wells, and luminescence measured following a 30 minute incubation to determine the degree of apoptosis following application of microdamage.

Statistics

All date was analysed for significance ($p \leq 0.05$) using one way ANOVA, post hoc Tukey test, to compare means.

Results

Figs 1: B, C and D show examples of the intact cell culture and an injury of 400 μm in phalloidin and DAPI stained gel embedded MLO-Y4 cells. The undamaged gel shows a homogenous distribution of cells, cells are completely absent in the region of the defect.

Effect of microdamage on RANKL and OPG release

Fig. 2 shows the effect of defect thickness on RANKL release measured using Enzyme linked immunosorbent assay (ELISA). There is no significant difference in RANKL release between negative control samples with cells and 160 μm samples over the 72 hours; however, a significant increase is seen in the 300 and 400 μm injury samples ($p \leq 0.05$). However, at 800 μm, a decrease in activity was observed in samples when compared to 300 and 400 μm samples.

As fig. 3 shows, OPG release was greatest in all groups compared to 400 μm samples. OPG release then peaked at 48 hours for all samples, however, again for the 400 μm injury size, release was significantly lower. A significant decrease in OPG release was subsequently seen at 72 hours in 400 μm samples. At 800 μm, release is comparable to smaller sized injuries, and is significantly less than 400 μm injuries ($p \leq 0.05$)**.**

Optimisation of transfection conditions in MLO-Y4 cells

Fig. 4 shows the luciferase activity of cells expressing the promoter construct with the luciferase gene downstream of the RANKL promoter compared to control cells. On stimulation of cells by 1,25 dihydroxyvitamin D3, luciferase activity showed a 2 fold increase in relative luciferase activity, 28 days following transfection, when compared to non transfected cells.

RANKL promoter activity

Fig. 5 shows the effect of microdamage on RANKL promoter activity. At 24 hours, promoter activity was seen to be greatest in 300 and 400 μm samples when compared to control 160 and 800 μm injury samples, with a significant increase being seen in the 400

μm sample. At 48 hours, a similar situation is noted, with the largest increase seen in 400 μm samples. At 72 hours, a highly significant increase in RANKL promoter activity occurred in both 300 and 400 μm samples, and the result for 160 μm just missed significance with a p value of 0.07. Again, the 800 μm injury size showed a decrease in RANKL production which is consistent with RANKL release. These results are broadly consistent with the ELISA results shown in fig.2, indicating significant effects of injury on RANKL production and release.

Effect of RANKL on entire undamaged cell populations

Fig.6 shows luciferase activity in populations of undamaged cell networks after application of conditioned media, i.e. media taken from injured networks in which the 400μm defect had been created. The results indicated a general tendency towards increasing RANKL with increasing time, though the only significantly different result was that in which the longest times were used (72hrs plus 72hrs).

Determination of cell viability following microdamage to gel embedded MLO-Y4 cells.

Fig.7 shows the effect of microdamage on cell viability and caspase 3 and 7 activity, and thus apoptosis, in gel embedded MLO-Y4 cells following microdamage. A significant decrease ($p \leq 0.01$) in cell viability was noted in 300 and 400 μm samples when compared to the control, 160 and 800 μm damaged samples (Fig 7.A),. Caspase 3 and 7 activity was measured to determine whether cells were apoptotic following microdamage (Fig 7.B). No significant difference was observed between control, 160, 300 and 800 μm samples, however, a significant increase in caspase activity was seen in 400 μm samples.

Discussion

Microdamage is one of the principal factors implicated in initiating the bone remodelling process [11]. Similar to fluid flow, microdamage is a natural occurrence linked to mechanical loading and accumulates following day to day wear and tear, yet levels of microdamage increase proportionally with age, hormonal status, and degree of loading on a bone [32, 33]. Bone remodelling is initiated in close proximity to microdamage, and so one could consider this to be an important mechanism utilised by bone to repair itself [34].

The present work has investigated, in much more detail than any previous study, the effect of planar, crack-like defects on the production by osteocyte-like cells of two cytokines which are crucial to the control of bone remodeling: RANKL and OPG. It is significant that no other mechanical stimulus was used beyond a single injury event and that this had measurable effects up to three days afterwards. Most studies concerned with the mechanical responses of osteocytes and other cells have shown that, in order to elicit significant responses, a repeated, cyclic application of the stimulus is required, be it matrix strain or fluid flow [26, 35, 36]. This is only to be expected because these cyclic events simulate repeated actions such as walking. In the case of microcracking, the damage remains in the bone until it is repaired, and it may grow over time, so its effective repair requires that it continue to be detected by the surrounding cells so long as the defect remains.

The present results showed a tendency to increased response (more RANKL and less OPG) with increased size of injury, except for the largest injury size which showed relatively little effect. Over a 72 hour time period, RANKL release remained relatively stable in control samples and 160 μm damaged samples. However, at 300μm damage, release of RANKL was two-fold higher than in control and 160μm samples. These results suggest that increase in microcrack size, up to a point (400 μm) causes a greater release of RANKL, with a plateau effect being noted between 48 and 72 hours. Additionally, a damage of 800 μm shows a RANKL release comparable to that of 160 μm, suggesting 300-400 μm defects to be the key damage size to cause cell process rupture and initiate the bone remodelling process. High levels of RANKL are indicative of bone resorption

and microdamage at early stages, and increased OPG secretion is associated with bone deposition and maintenance of bone structure *in vivo* [14].

OPG release tends to inversely correspond with RANKL release in most samples. Release generally remains consistent in control samples and in samples below 300 μm. At 400 μm, release of OPG is significantly lower than what is seen in small sized injuries. This correlates with RANKL release being highest at 400 μm at all time points. Moreover, this may be suggestive of the binding and sequestering of RANKL by OPG and a lack of sufficient signals being released to trigger OPG production.

The increasing effect is most likely due to the increased numbers of cells being affected - the cells were approximately 100μm apart so the thicker wires would have encountered more cells and more processes – and also the reduced tendency for thicker defects to heal. Future studies are planned in which the integrity of cells and processes around the injury sites are examined using detailed microscopy. At present there is no clear explanation for the anomalous effect of the 800μm wire: a possible explanation is that this was thick enough to cause rupture and necrosis of large numbers of cells (as opposed to processes) and thus to initiate a completely different set of responses.

This work is consistent with many previous findings which have linked microdamage to remodeling [11, 34, 37] and which have suggested that individual microcracks can be detected by the surrounding cells which can signal to initiate the repair response [38, 39]. The present results correlate with the hypotheses of Hazenberg *et al* 2006 [28], among previous studies, which suggested that RANKL and OPG release, and ultimately, bone remodelling, was injury size dependant [28, 30], and indeed that microdamage manifests its effects through cellular disruption [28]. However, more work is required before this mechanism can be confirmed.

Examination of the effect of microdamage on a non-injured cell population has allowed for clarification as to whether the cells, having undergone process rupture as a result of microdamage, signal for a response to damage from surrounding cells. This may have shown that, in spite of an injured cell's impaired viability, microdamage may still be able to be repaired by a BMU through the recruitment of a neighboring cell response. Additionally, assessment of cell viability and apoptosis within our model has provided

data to further elucidate some of the cellular responses to microdamage. The results have shown that cell viability remains unaffected in control and small defect sizes; however, a significant decrease in cell viability occurs at 300 and 400 μm defect sizes, only to then return to normal levels at 800 μm. Regarding apoptosis levels, Caspase 3 and 7 activity remained consistent in control and 160 μm defects, and then significantly increases at 400 μm. These results are consistent with the increased release of RANKL and decrease in OPG release at 72 hours in 300 and 400 μm, and furthermore demonstrate the similar behavior of cells to large and small damage size (160 & 800μm).

A limitation of the present study was that the defects created, though they were similar to cracks in shape, were much larger than cracks normally encountered in bone *in vivo*. This was dictated by the resolution of our methods for the measurement of RANKL and OPG, which required relatively large numbers of cells to be involved. However, it is necessary to consider that there are some differences in morphology between the MLO-Y4 cells in our experiment and real osteocytes in bone. We found that our cells have an average of 13 processes per cell, whereas there are approximately 50 processes per osteocyte in vivo [40]. Furthermore, in this model, cell spacing, with 1×10^6 cells per mL gel, is 100 μm. In vivo, the density of osteocytes is 12,000-20,000 per mm^2 [41], giving a spacing of 37 μm between cells. One can estimate the number of processes which will cross a crack of given size, both in our experiment and in bone. This calculation shows that number of processes spanning the crack in our experiment, 10,833, would be the same as the number spanning a crack in bone of transverse length 500μm. This would be at the upper end of the lengths of cracks which actually exist: a more typical *in vivo* crack length is 100μm. This shows that, whilst we do need to refine our experiment somewhat, it is already close to the *in vivo* situation.

It is hoped to refine the experiment in future to enable smaller numbers of cells, and smaller defects, to be studied. This limitation can be overcome to some extent by the development of a theoretical model, which will allow us to predict the responses to microcracks of realistic size. Early data (not presented) using a model have been very encouraging: they showed that cracks of the typical length found in bone (100μm) would

be expected to generate RANKL levels different from the background levels in cases where the applied stress was relatively high, but that at lower stresses a larger crack length would be needed. This implies that the cell network would be able to detect only those cracks which are potentially dangerous, i.e. which are likely to grow to cause stress fractures.

Conclusion

In conclusion, this study has demonstrated that injury size could be critical in affecting the instigation of bone remodelling and that the subtle difference between damage and failure may have implications in bone repair. The study also shows that microdamage may be a principal mediator of bone remodelling through its effect on RANKL release and may confirm the reason as to why small cracks are left unrepaired in bone in vivo.

Acknowledgements

This work was funded by Science Foundation Ireland under the Research Frontiers Programme grant number RFP-ENM-991. The MLO-Y4 cells were generously provided by Dr. Linda Bonewald (School of Dentistry, University of Missouri, Kansas City, MO.). The promoter construct was kindly donated by Dr Charles O Brien (University of Arkansas for Medical Sciences. 4301 W. Markham St. ACRC 834. Little Rock, AR 72205)

References

[1] D.L. Lacey, E. Timms, H.L.Tan, H.L, Osteoprotegerin ligand is a cytokine that regulates osteoclast differentiation and activation, *Cell* **93** (1998) pp 165-176.
[2] W.S. Simonet, D.L. Lacey, C.R. Dunstan, M. Kelley, M.S. Chang, R. Luthy, H.Q. Nguyen, S. Wooden, L. Bennett, T. Boone, G. Shimamoto, M. DeRose, R. Elliott, A. Colombero, H.L. Tan, G. Trail, J. Sullivan, E. Davy, N. Bucay, L. Renshaw-Gegg, T.M. Hughes, D. Hill, W. Pattison, P. Campbell, W.J. Boyle, Osteoprotegerin: a novel secreted protein involved in the regulation of bone density, *Cell* **89** (1997) pp 309-319.
[3] J.M. Hayden, S. Mohan, D.J. Baylink, The insulin-like growth factor system and the coupling of formation to resorption, *Bone* **17** (1995) pp 93-98.
[4] C. Zhao, N. Irie, Y. Takada, K. Shimoda, T. Miyamoto, T. Nishiwaki, T. Suda, K. Matsuo, Bidirectional ephrinB2-EphB4 signaling controls bone homeostasis, *Cell* **2** (2006) pp 111-121.
[5] H.K. Vaananen, Zhao, M, and Mulari, M. , The cell biology of osteoclast function, *J. Cell. Sci.* **113** (2000) pp 377-381.
[6] Y. Kato, J.J. Windle, B.A. Koop, G. Mundy, L.F. Bonewald, Establishment of an Osteocyte-like Cell Line, MLO-Y4, *J.Bone Miner.Res.* **12** (1997) pp 2014-2023.
[7] L.F. Bonewald, Osteocytes as dynamic multifunctional cells, *Ann N Y Acad Sci* **1116** (2007) pp 281-290.
[8] J. Klein-Nulend, C.M. Semeins, N.E. Ajubi, P.J. Nijweide, E.H. Burger, 1995 217:64064, Pulsating fluid flow increases nitric oxide (NO) synthesis by osteocytes but not periosteal fibroblasts-Correlation with prostaglandin upregulation *Biochem Biophys Res Commun* **217** (1995) pp 640-647.
[9] M. Schaffler, K. Choi, C. Milgrom, Ageing and matrix microdamage accumulation in human and compact bone, *J.Bone Miner.Res.* **15** (1995) pp 60-67.
[10] B.S. Noble, J. Reeve, Osteocyte function, osteocyte death and bone fracture resistance, *Mol. Cell. Endocrinol.* **159** (2000) pp 7-13.
[11] D.B. Burr, R.B. Martin, M. Schaffler, E.L. Radin, Bone remodeling in response to in vivo fatigue microdamage, *J.Biomech* **18** (1985) pp 189-200.
[12] T.C. Lee, A. Staines, D. Taylor, Bone adaptation to load: microdamage as a stimulus for bone remodelling, *J. Anat.* **201** (2002) pp 437-446.
[13] P.J. Prendergast, D. Taylor, Prediction of bone adaptation using damage accumulation, *J. Biomech.* **27** (1994) pp 1067-1076.
[14] A.G. Robling, A.B. Castillo, C.H. Turner, Biomechanical and molecular regulation of bone remodeling, *Annu RevBiomed Eng* **8** (2006) pp 455-498.
[15] L. Lum, B.R.Wong, R. Josien, J.D. Becherer, H. Erdjument-Bromage, J. Schlondorff, (1999) . Evidence for a role of a tumor necrosis factor-alpha (TNF-alpha)-converting enzyme-like protease in shedding of TRANCE, a TNF family member involved in osteoclastogenesis and dendritic cell survival., *J Biol Chem* **274** (1999) pp 13613-13618.
[16] H. Yasuda, N. Shima, N. Nagakawa, Osteoclast differentiation factor is a ligand for osteoprotegrin osteoclastogenesis-inhibitory factor and is identical to trance/RANKL, *Proc Natl Acad Sci USA* **95** (1998) pp 3597-3602.

[17] B.O. Oyajobi, D.M. Anderson, K. Traianedes, P.J. Williams, T. Yoneda, G. Mundy, Therapeutic Efficacy of a Soluble Receptor Activator of Nuclear Factor {kappa}B-IgG Fc Fusion Protein in Suppressing Bone Resorption and Hypercalcemia in a Model of Humoral Hypercalcemia of Malignancy, *Cancer Res* **61** (2001) pp 2572-2578.
[18] K.J. Walton, J.M. Duncan, P. Deschamps, S.G. Shaughnessy, Heparin acts synergistically with interleukin-11 to induce STAT3 activation and in vitro osteoclast formation, *J. Theor. Biol.* **100** (2002) pp 2530-2536.
[19] G. Kalliolias, B. Zhao, A. Triantafyllopolou, K.H.P. Min, L.B. Ivashkiv, Interleukin 27 inhibits human osteoclastogenesis by abrogating RANKL-mediated induction of nuclear factor of activated T cells c1 and suppressing proximal RANK signaling. , *Rheumatoid Arthritis Basic Science Studies* **62** (2010) pp 402-411.
[20] B.G. Darnay, V. Haridas, J, Ni, P.A. Moore, B.B. Aggarwal, Tumor necrosis factor receptor family member RANK mediates osteoclast differentiation and activation induced by osteoprotegerin ligand, *J.Biol.Chem.* **273** (1998) pp 20552-20555.
[21] W.J. Boyle, W.S. Simonet, D.L. Lacey, Osteoclast differentiation and activation., *Nature* **473** (2003) pp 337-342.
[22] T.L. Burgess, Y. Qian, S. Kaufman, B.D. Ring, G. Van, C. Capparelli, M. Kelley, H. Hsu, W.J. Boyle, C.R. Dunstan, S. Hu, D.L. Lacey, The ligand for osteoprotegerin (OPGL) directly activates mature osteoclasts, *J. Cell. Biol* **145** (1999) pp 527-538.
[23] B.R. Wong, J. Rho, J. Arron, E. Robinson, J. Orlinick, M. Chao, S. Kalachikov, E. Cayani, F.S. Bartlett, W.N. Frankel, S.Y. Lee, Y. Cho, TRANCE is a novel ligand of the tumor necrosis factor receptor family that activates c-*jun* N-terminal kinase in T cells, *J. Biol. Chem.* **272** (1997) pp 25190-25194.
[24] P.J. Bekker, D. Holloway, A. Nakanishi, The effect of a single dose of osteoprotegrin in postmenopausal women., *J Bone Miner Res* **16** (2001) pp 348-360.
[25] X. Cheng, M. Kinosaki, M. Takami, Y. Choi, H. Zhang, R. Murali, Disabling of Receptor Activator of Nuclear Factor-_B (RANK) Receptor Complex by Novel Osteoprotegerin-like Peptidomimetics Restores Bone Loss in Vivo, *J.Biol.Chem.* **9** (2004) pp 8267-8277.
[26] C.H. Turner, M.R. Forwood, M.W. Otter, Mechanotransduction in bone: do bone cells act as sensors of fluid flow?, *FASEB J* **8** (1994) pp 875-878.
[27] D. Taylor, J.G. Hazenberg, T.C. Lee, The cellular transducer in damage stimulated remodelling: a theoretical investigation using fracture mechanics. *J. Theor. Biol*, **225** (2003) pp 65-75.
[28] J.G. Hazenberg, D. Taylor, T.C. Lee, Mechanisms of short crack growth at constant stress in bone, *Biomater,* **9** (2006) pp 2114-2122.
[29] J.G. Hazenberg, T.A. Hentunen, T.J. Heino, K. Kurata, T.C. Lee, D. Taylor, Microdamage detection and repair in bone: Fracture Mechanics, histology, cell biology, *Technol Healthcare* **17** (2009) pp 67-75.
[30] K. Kurata, T.J. Heino, H. Higaki, H.K. Vaananen, Bone marrow cell differentiation induced by mechanically damaged osteocytes in three dimensional gel embedded culture, *J.Bone Miner.Res.* **4** (2006) pp 616-625.
[31] C.A. O' Brien, B. Kern, I. Gubrij, G. Karsenty, S.C. Manolagas, Cbfa1 does not regulate RANKL gene activity in stromal/osteoblastic cells, *Bone* **30** (2002) pp 453-462.

[32] O. Verborgt, G.J. Gibson, M.B. Schaffler, Loss of osteocyte integrity in association with microdamage and bone remodeling after fatigue in vivo, *J Bone Miner Res* **15** (2000) pp 60-67
[33] S. Mori, D.B. Burr, Increased intracortical remodeling following fatigue damage, *Bone* **14** (1993) pp 103-109.
[34] R.B. Martin, Fatigue Damage, Remodeling, and the Minimization of Skeletal Weight. , *J. Theor. Biol.* **220** (2001) pp 271-276.
[35] E.H. Burger, J. Klein-Nulend, T.H. Smith, Strain derived canalicular fluid flow regulated osteoclast activity in a remodeling osteon - a proposal, *Journal of Biomechanics* **10** (2003) pp 1453-1459.
[36] A.G. Robling, A.B. Castillo, C.H. Turner, Biomechanical and molecular regulation of bone remodeling, *Annu Rev Biomed Eng* **8** (2006) pp 455-498.
[37] R.B. Martin, On the histologic measurement of osteonal BMU activation frequency, *Bone* **15** (1994) pp 547-549.
[38] R.B. Martin, A theory of fatigue damage accumulation and repair in cortical bone, *J. Ortho. Res.* (1992) pp 818-825.
[39] D. Taylor, P.J. Prendergast, Damage accumulation in compact bone - a fracture mechanics approach to estimate damage and repair rates, *Adv Bioeng* **13** (1995) pp 337-338.
[40] J.G. Hazenberg, D. Taylor, T.C. Lee, The role of osteocytes and bone microstructure in preventing osteoporotic fractures, *Osteoporos Int* **18** (2007) pp 1-8.
[41] R.B. Martin, D.B. Burr, Structure, Function and Adaptation of Compact Bone, *New York, Raven Press* (1989) pp 275

Figure Legends:

Figure 1: Application of microdamage to 3D gel embedded MLO-Y4 cells.A: Device used to apply planar defect to 3D collagen-matrigel embedded MLO-Y4 cells. B. 10X micrograph of phalloidin stained 3D gel embedded MLO-Y4 cells (phalloidin-green- f actin in cytoskeleton). C. 40X micrograph of Phalloidin and DAPI stained gel embedded MLO-Y4 cells (DAPI- blue- nucleus). D:10X Micrograph of 160 µm injury interface in 3D gel embedded MLO-Y4 cells.

Figure 2: The effect of varying microdamage size on RANKL release from 3D gel embedded MLO-Y4 cells. Results show RANKL release as quantified by ELISA. A significant increase ($P \leq 0.05$) in RANKL release was seen in the 400 micron samples when compared to controls and other injury samples at 24 hours. In the 48 and 72 hour groups, both 300 and 400 micron samples showed a significant increase in RANKL production when compared to other samples within the group ($P \leq 0.05$). * indicates $P \leq 0.001$ when comparing 24 negative control data to other data within the experimental group. **denotes $p \leq 0.05$ significance of 400 µm data to other samples at 24 hours, # denotes significant of 0.05 when comparing 300 and 400 µm samples to other groups at 48 and 72 hour time points. Error bars are indicative of standard deviation, n = 9.

Figure 3: The effect of varying microdamage size on OPG release from 3D gel embedded MLO-Y4 cells. Results show OPG release as quantified by ELISA. A significant increase ($P \leq 0.05$) in OPG release was initially seen in both control and injured sample. 48 hours post injury, a statistically significant increase in OPG is noted in all samples when compared to 24 hours, however, this decreases significantly in all samples at 72 hours ($P \leq 0.05$). ***** indicates $P \leq 0.001$ when comparing negative control data to all other data, ** denotes $p \leq 0.05$ when comparing significance within a group at a specific time point. # denotes significance to same injury size compared to 24 hours and 72 hours. Error bars are indicative of standard deviation, n = 9.

Figure 4: Luciferase assay of MLO-Y4 cells expressing RANKL promoter construct with the luciferase gene downstream of the RANKL promoter compared to control cells. On stimulation of 1nM 1,25 dihydroxy Vitamin D3, Luciferase assay displayed a 2 fold increase in relative luciferase activity, 28 days post transfection, when compared to non transfected MLO-Y4 cells ($P = 0.04$). * denotes $p \leq 0.04$ when comparing transfected cells to control cells.

Figure 5: Microdamage causes an increase in RANKL production. Results show the effect of varying size microdamage on RANKL production in gel embedded MLO-Y4 cells. Results show RANKL production as quantified by Luciferase assay. Luciferase assay showed increase in RANKL activity over time in microdamage samples. Production of RANKL was found to be significantly highest in samples with greater damage (300 and 400 microns) at 72 hours ($P \leq 0.05$). * denotes $p \leq 0.05$ showing significance in increase in luciferace activity at 400 µm at 24 hours. # indicates $p \leq 0.05$,

showing 300 and 400 μm at 72 hours being significantly greater than the same injury size at 24 and 48 hours Error bars are indicative of standard deviation, n = 9.

Figure 6: The effect of microdamage on entire cell population. Luciferase activity was used to quantify RANKL promoter activity 72 hours after microdamage on cells surrounding injury. Conditioned media from previous experiments 48 hours post injury showed an insignificant increase in RANKL production at all time points when compared to the control. Conditioned media from previous experiments 72 hours post injury showed an insignificant increase in RANKL production at all time points when compared to the control at 24 and 48 hours. At 72 hours, a 2 fold increase was noted when compared to all other samples. * denotes $p \leq 0.05$ when comparing a significant increase in luciferase activity at 72 hours following microdamage and after 72 hours of treatment.

Figure 7: The effect of microdamage on cell viability, cytotoxicity and apoptosis in MLO-Y4 cells following microdamage. A significant decrease ($p \leq 0.01$) in cell viability was noted in 300 and 400 μm samples when compared to the control, 160 and 800 μm damaged samples. No significant difference was observed in cytotoxicity in control, 160, 300 and 400 μm samples; however, a significant decrease (* $p \leq 0.05$) in cytotoxicity was noted in 800 μm samples. No significant difference was observed between control, 160, 300 and 800 μm samples with regard to apoptosis. A significant increase in caspase activity was seen in 400 micron samples when compared to the control, 160 and 300 μm samples. * denotes $p \leq 0.01$ when comparing 300 and 400 μm samples to all other samples. ** denotes $p \leq 0.01$ when comparing 400 μm sample to other samples.

Figure 1

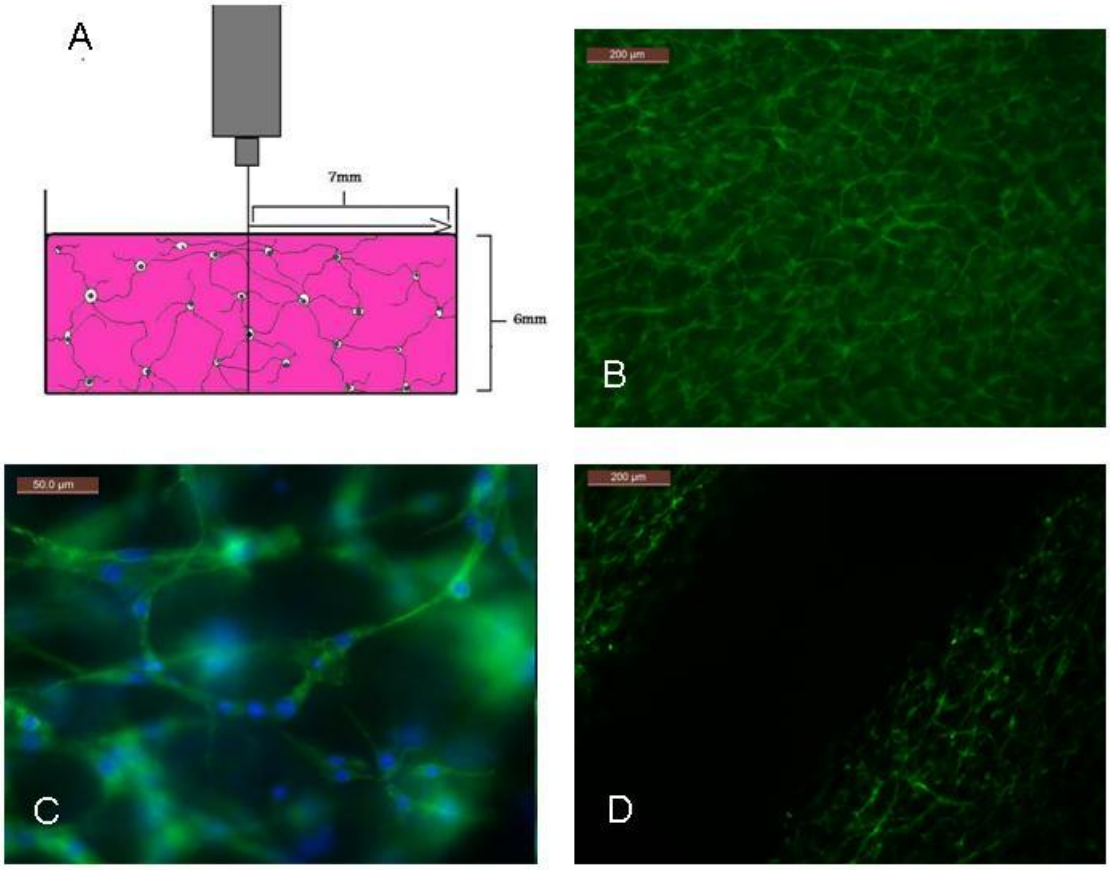

Figure 2

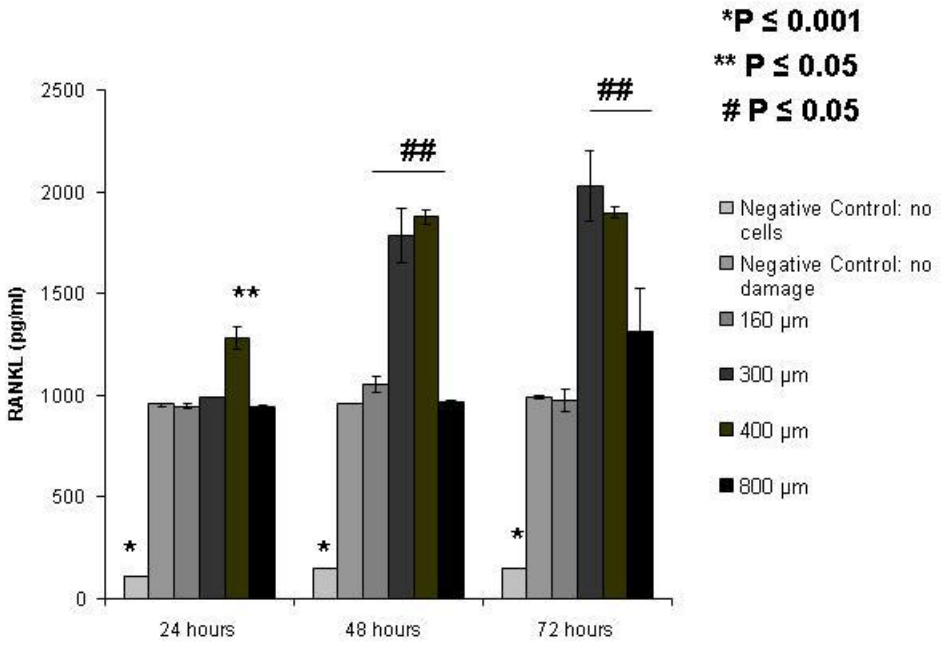

Figure 3

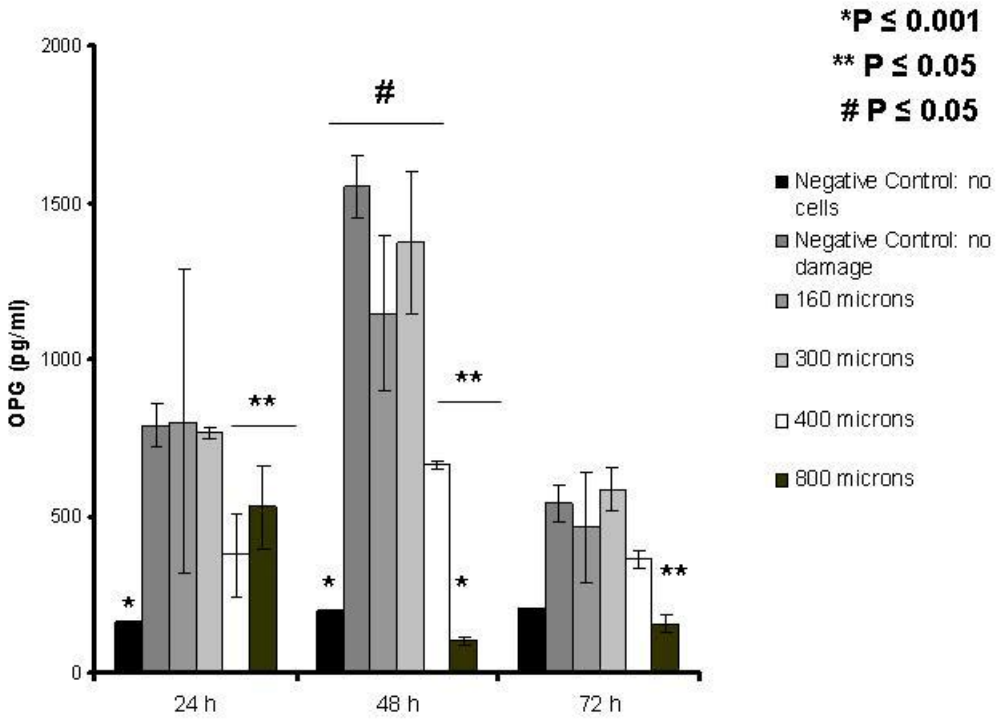

Figure 4

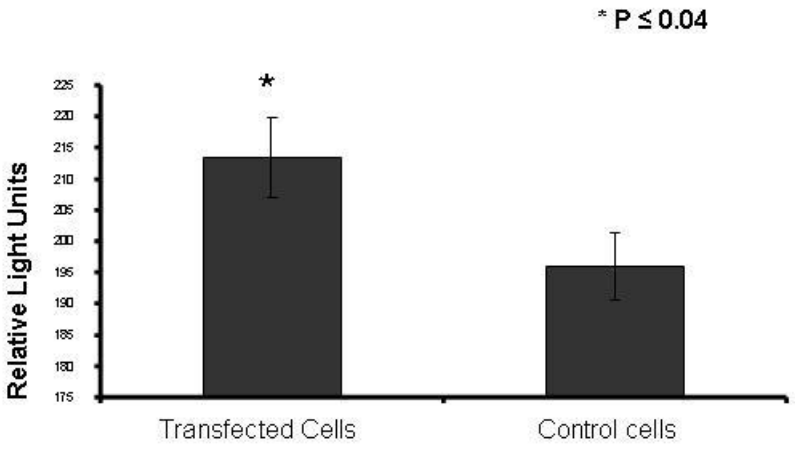

Figure 5

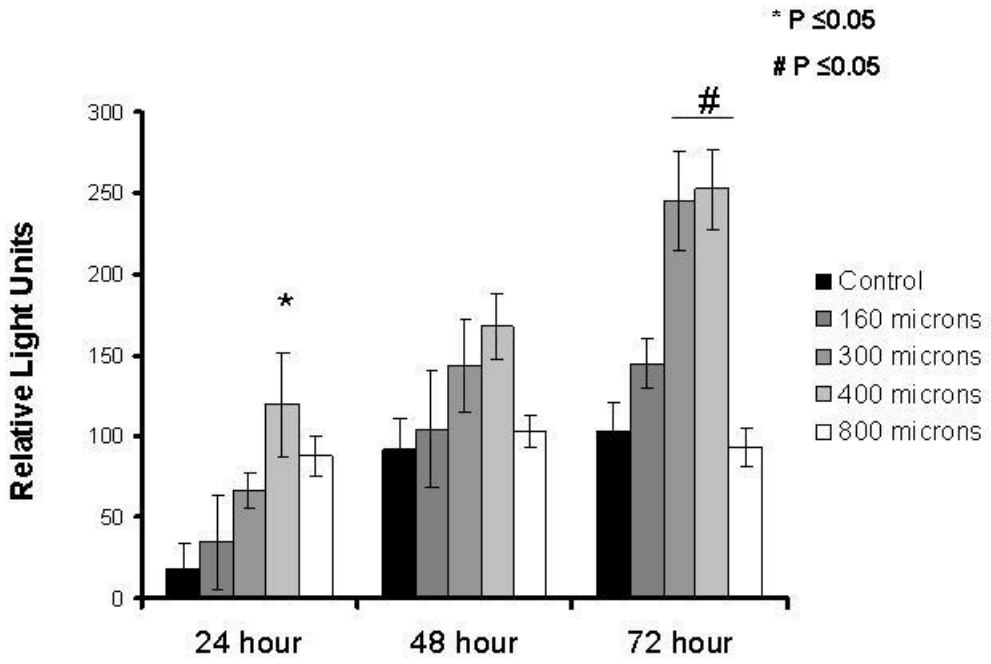

Figure 6

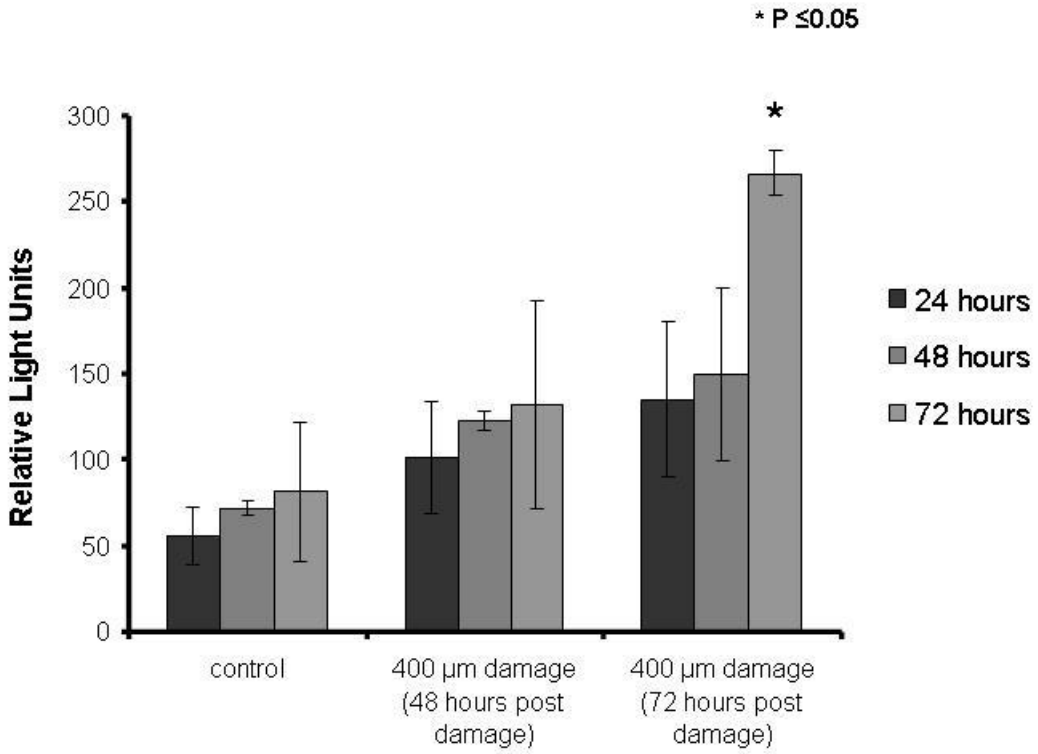

Figure 7

A

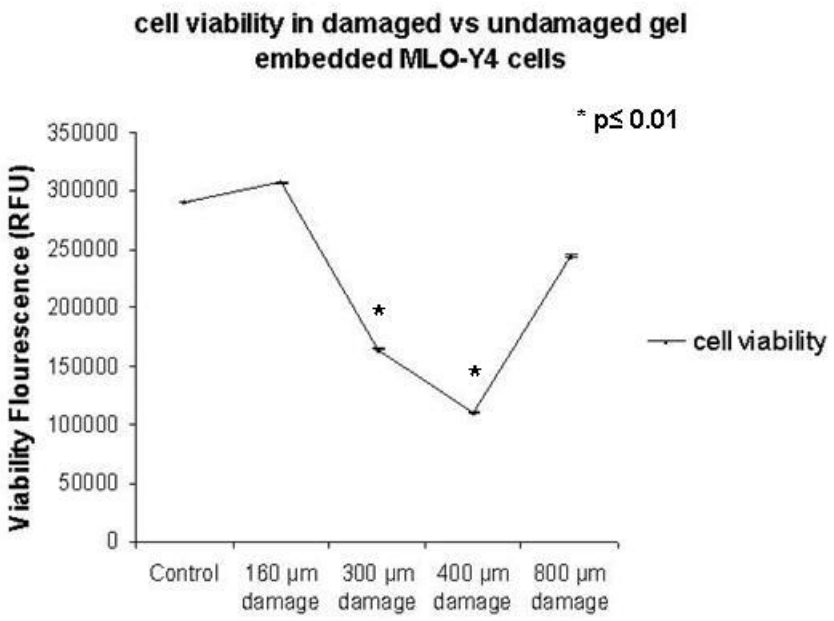

B